IEEE Access
Multidisciplinary | Rapid Review | Open Access Journal

SPECIAL SECTION ON EMERGING TRENDS, ISSUES AND CHALLENGES FOR ARRAY SIGNAL PROCESSING AND ITS APPLICATIONS IN SMART CITY

Received December 31, 2019, accepted January 15, 2020, date of publication January 21, 2020, date of current version January 29, 2020.

Digital Object Identifier 10.1109/ACCESS.2020.2968382

Gear Fault Diagnosis Based on Genetic Mutation Particle Swarm Optimization VMD and Probabilistic Neural Network Algorithm

JIAKAI DING[1], DONGMING XIAO[1,2], AND XUEJUN LI[1,2]

[1]Hunan Provincial Key Laboratory of Health Maintenance for Mechanical Equipment, Hunan University of Science and Technology, Xiangtan 411201, China
[2]School of Mechatronics Engineering, Foshan University, Foshan 528225, China

Corresponding author: Dongming Xiao (dongming.xiao@outlook.com)

This work was supported by the National Natural Science Foundation of China under Grant 51875195 and Grant 51875196.

ABSTRACT The decomposition number K and penalty factor α in the variational mode decomposition (VMD) algorithm have a great influence on the decomposition effect and the accuracy of subsequent fault diagnosis. Therefore, a gear fault diagnosis method based on genetic mutation particle swarm optimization VMD and probabilistic neural network (GMPSO-VMD-PNN) algorithm is proposed in this paper. Firstly, the GMPSO algorithm is used to optimize the $[K, \alpha]$ parameter combination in the VMD algorithm, and the optimal $[K, \alpha]$ parameter combination of each gear fault vibration signal to be decomposed is selected. Then, the gear fault vibration signal is decomposed into several intrinsic mode functions (IMFs) by VMD, and the sample entropy value of each IMFs is extracted to form the feature vector of subsequent fault diagnosis. Finally, the characteristic vector of gear fault vibration signal is input into PNN model, and gear fault is accurately classified. By comparing with fixed parameter VMD algorithm, empirical mode decomposition (EMD) and complete ensemble empirical mode decomposition adaptive noise (CEEMDAN) algorithm, the superiority of this method in gear fault diagnosis is verified. Therefore, the GMPSO-VMD-PNN algorithm proposed in this paper has certain application value for gear fault diagnosis.

INDEX TERMS Genetic mutation particle swarm optimization, variational mode decomposition, probabilistic neural network, gear fault diagnosis, parameter optimization.

I. INTRODUCTION

Gearbox play a very important role in the mechanical transmission system [1] and are widely used in wind turbines, power transmission machinery and other equipment [2]–[5]. The gear often suffers from such defects as wear, cracks and broken teeth [6]–[8]. When these faults occur to the gear parts in the gearbox, they will cause serious harm to the operating mechanical system [9]. Therefore, fault diagnosis of gear parts in gearbox is beneficial to prevent excessive damage of mechanical system, and has a certain positive impact on preventing mechanical system safety.

Time-frequency analysis based on vibration signals has been successfully applied to gear fault diagnosis [10]–[16], whose gear fault vibration signals contain problem information generated during the operation of the gearbox. Therefore, the analysis of gear fault vibration signal is the premise of gear fault diagnosis. Gear fault diagnosis uses not only vibration signals, but also new technologies such as acoustic signals and acoustic emission signals [17]–[19], and the combination of these new technologies can improve the accuracy of gear fault diagnosis [20]. In the field of gear vibration signal fault diagnosis, there are several commonly used methods. For example, continuous wavelet transform (CWT) [21], [22], Hilbert-Huang transform (HHT) [23], [24], empirical mode decomposition (EMD) [25], [26], ensemble empirical mode decomposition (EEMD) [27], [28] and local mode decomposition (LMD) [29], [30], etc. However, the effect of continuous wavelet transform is based on the selection of wavelet basis function. Once the wavelet basis function is determined, the decomposition mode is also determined. We need to select different wavelet basis functions to analyze different gear vibration signals, which will increase the artificial efficiency of the decomposition process. In the decomposition process of EMD, EEMD and LMD, there are some adverse effects such as mode mixing and endpoint

The associate editor coordinating the review of this manuscript and approving it for publication was Liangtian Wan.

effect [31]–[34]. Therefore, Dragomiretskiy [35] proposed an adaptive signal decomposition algorithm called variational mode decomposition (VMD), which can overcome the adverse effects such as mode confusion and endpoint effect of EMD, EEMD and LMD. Li *et al.* [36] proposed a data-driven time-frequency analysis (DDTFA) method. Firstly, VMD was used to carry out adaptive decomposition of signals, which resulted in high frequency accuracy and good noise resistance of each intrinsic mode functions (IMFs). The conclusion is that the VMD algorithm can also decompose the required signal in the environment of strong noise and has strong adaptability. Hu *et al.* [37] proposed an algorithm based on VMD and detrended fluctuation analysis (DFA) to diagnose gear faults in heavy duty gearboxes. The original signal was adaptively decomposed into several IMFs by VMD, and then the peak value and correlation coefficient of each IMFs were extracted to describe the characteristics of the signal. Finally, experiments show that this method can effectively improve the accuracy of gear fault diagnosis. Li *et al.* [38] also used the VMD algorithm to carry out adaptive decomposition of signals, and used the improved kernel extreme learning machine (KELM) to diagnose rolling bearing faults. At the same time, they also compared with BP neural network (BPNN), support vector machine (SVM) and traditional ELM, and the results showed that this method was better than other methods in fault diagnosis accuracy. Li *et al.* [39] proposed to combine VMD with coupled underdamped stochastic resonance (CUSR) to extract shock fault characteristics of gearbox. The results show that this method can effectively extract the characteristics of gearbox impact fault.

However, the decomposition effect of VMD algorithm depends on the selection of decomposition parameters, such as the decomposition number K and penalty factor α [40]. The parameter optimization of VMD algorithm is mainly aimed at the two parameters of the decomposition number and penalty factor. The method is to optimize the decomposition number or the combination of these two parameters by using the intelligent optimization algorithm to obtain the optimal parameter value [6], [41], [42]. Xiao *et al.* [6] proposed an instantaneous frequency mean value as the basis for selecting the decomposition number K in the VMD algorithm, and used the unsupervised learning algorithm self-organizing map (SOM) neural network to classify gear faults and compare with EMD. The accuracy of gear fault diagnosis is much higher than that of EMD algorithm. Wang *et al.* [43] proposed an adaptive parameter optimized VMD (APOVMD) algorithm, which can self-adaptively and non-recursively decompose planetary gearbox vibration signals into several IMFs. Finally, compared with VMD and EEMD algorithms, the ability to extract early weak fault characteristics of planetary gearbox is compared. Yan and Jia [44] proposed an cuckoo search algorithm-based variational mode decomposition (CSA-VMD) considering that the internal parameters in the VMD algorithm need to be set in advance, in which the CSA algorithm can search the optimal value of the internal parameters of the VMD according to the objective function. Zhang *et al.* [45] used grasshopper optimization algorithm (GOA) to optimize the combination of the decomposition number K and penalty factor α parameters in the VMD algorithm, and selected the maximum weighted kurtosis index as the optimization target to select the optimal parameter combination. An example is given to prove that the method can effectively analyze mechanical vibration signals and be used for fault diagnosis. Yi *et al.* [46] proposed a fault feature extraction method based on particle swarm optimization (PSO) to optimize VMD. Compared with traditional envelope spectrum analysis, this method is superior to EMD algorithm in complex signal decomposition. However, PSO algorithm is prone to local minima, so PSO algorithm has to be improved to achieve the best results.

In recent years, researchers have done a lot of research on fault diagnosis algorithms. In terms of gear fault diagnosis, its fault diagnosis algorithms mainly include SVM [47], [48], neural network (NN) [6], [49], [50] and the emerging deep neural network (DNN) technology [51], [52]. Liu [53] pointed out in the paper that the SVM algorithm also needs to select the internal parameters well when performing fault diagnosis. Different parameters have different effects and uncertainties. Xiao *et al.* [6] proposed a gear fault diagnosis method based on the combination of VMD and SOM neural network. The SOM neural network is an unsupervised learning algorithm, which can adaptively classify the extracted feature vectors until the gear fault category is separated. Compared with SVM algorithm, the accuracy of neural network is higher than that of SVM algorithm, and there is no need to select internal parameters in advance. It can self-adapt to classify feature vectors. Specht [54] proposed a probabilistic neural network (PNN), which is a parallel algorithm based on Bayes classification rules and the probability density function estimation method of Parzen window. PNN is a supervised learning neural network and is widely used in pattern recognition and fault diagnosis. Liu *et al.* [55] proposed a VMD and PNN based on the Electromechanical actuators (EMAs) fault diagnosis method, the experimental results show that the method can work under weak conditions of realization of EMAs fault diagnosis effectively. Marugán *et al.* [56] pointed out in the paper that PNN has been widely used in the field of fault diagnosis and has a very promising application prospect.

Based on the studies in the above literatures, the problems such as mode mixing and endpoint effect of EMD and LMD algorithms, local minima of PSO algorithms, and the need to set internal parameters of SVM in advance are addressed. A gear fault diagnosis algorithm based on genetic mutation particle swarm optimization VMD and probabilistic neural network (GMPSO-VMD-PNN) algorithm is proposed in this paper. Among them, the GMPSO algorithm can effectively avoid the local minimum value of PSO algorithm, and then apply GMPSO to the $[K, \alpha]$ combination parameter optimization problem of VMD algorithm. The optimal value of $[K, \alpha]$ combined parameters can be effectively obtained to perform VMD decomposition of gear fault vibration signal, which can effectively avoid the occurrence of mode mixing

FIGURE 1. Experimental system: (1) laptop, (2) B&K data acquisition analyzer, (3) coupling, (4) acceleration sensor, (5) reducer, (6) coupling, (7) three-phase induction motor, and (8) electromagnetic speed control motor controller.

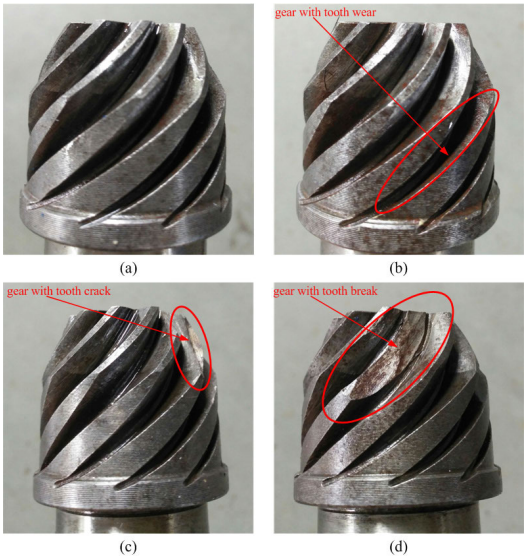

FIGURE 2. (a) Normal gear, (b) gear with tooth wear, (c) gear with tooth crack, and (d) gear with tooth break.

and endpoint effect. Finally, PNN is used for fault diagnosis to effectively improve the accuracy of gear fault diagnosis.

II. EXPERIMENT AND THE PROCEDURE

A. EXPERIMENTAL SYSTEM AND DATA ACQUISITION

In order to verify the effectiveness of the proposed GMPSO-VMD-PNN algorithm in gear fault diagnosis, a spiral bevel gear test rig was established and tested. The experimental system is shown in Figure 1. The test rig includes laptop (1), data acquisition analyzer (B&K, Type 3053-b120, B&K company, Denmark) (2), coupling (3), acceleration sensor (4), reducer (5) (Shanghai Nini reducer Co., Ltd, Shanghai, China), coupling (6), three-phase asynchronous motor (7), electromagnetic speed-regulating motor controller (8) (Shanghai Shanchuang instrument & meter Co., Ltd, Shanghai, China). The three-phase asynchronous motor (7) for driving. The reducer (5) is connected to the output shaft by a coupling (3), and the speed of the three-phase asynchronous motor (7) is controlled by a speed controller, which can operate the reducer (5) to be tested at various speeds. The reducer (5) is driven by three-phase asynchronous motor (7) through coupling (6). The rated power output of three-phase asynchronous motor (7) is 1.1kW. Among them, the electromagnetic speed-regulating motor controller (8) allows manual adjustment of load torque. The vibration signal of the reducer (5) is collected by the acceleration sensor (4), which adopts 4514b-001 acceleration sensor (4) produced by B&K company in Denmark. Among them, the acceleration sensor (4) output is sent to laptop (1) through data acquisition analyzer (2). The acceleration sensor (4) layout position is at the output shaft of gear reducer (5). The B&K data acquisition analyzer (2) is used to collect the vibration signals of the gears when it is, so as to simulate the deterioration process of gear fault. The failure parts of normal gear, gear with tooth wear, gear with tooth crack and gear with tooth break in the spiral bevel gear test rig is shown in Figure 2.

In this paper, normal gear, gear with tooth wear, gear with tooth crack and gear with tooth break under four conditions were analyzed. Among them, the sampling frequency of gear vibration signal is 8192Hz, the acquisition duration of each signal is 0.25s, and a total of 16 segments of data are collected.

B. FAULT DIAGNOSIS BASED ON GMPSO-VMD-PNN ALGORITHM

The vibration signal of gearbox provides a lot of information for the fault diagnosis of gear. When the gear fails, the vibration signal generated during the operation of gearbox will change greatly. Therefore, it is necessary to build a detection platform to monitor and record the vibration signal of gearbox under different working conditions. However, in the monitoring process, there are a lot of noise signals in the original monitoring data. In order to effectively extract the vibration signal characteristics of gear fault, a gear fault diagnosis method based on GMPSO-VMD-PNN is proposed in this paper, and its flow chart is shown in Figure 3.

The specific steps are as follows:

Step 1. According to a certain sampling frequency f_s, vibration signals of gear under four working conditions of normal gear, gear with tooth wear, gear with tooth crack and gear with tooth break for N times were collected, with a total of 4N samples;

Step 2. The parameter combination $[K, \alpha]$ of VMD was optimized with GMPSO;

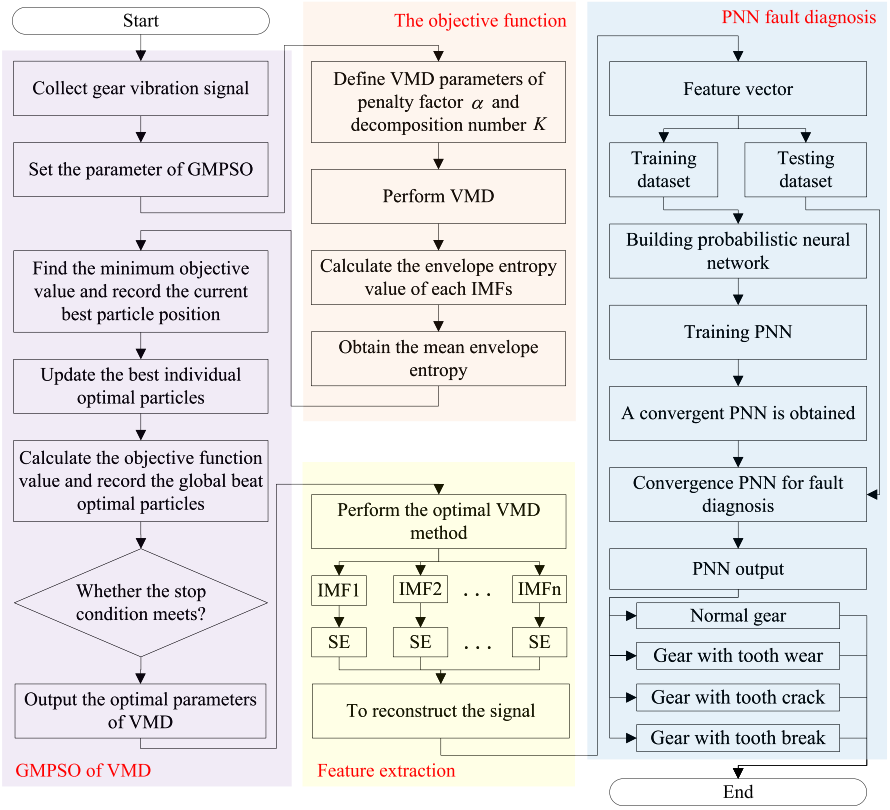

FIGURE 3. Gear fault diagnosis flow chart based on genetic mutation particle swarm optimization variational mode decomposition and probabilistic neural network (GMPSO-VMD-PNN).

Step 3. VMD decomposition was carried out for each vibration signal, and a total of K IMFs were decomposed;

Step 4. Extract the sample entropy value of each IMFs to form the feature vectors;

Step 5. Input the feature vectors to PNN for fault diagnosis;

Step 6. Output fault diagnosis results and make comparative analysis.

III. BASED ON THE SAMPLE ENTROPY GMPSO-VMD GEAR FAULT FEATURE EXTRACTION METHOD

The VMD algorithm was proposed by Dragomiretskiy and Zosso in 2014 [35]. The VMD algorithm decomposes the collected gear vibration signal $x(t)$ by constructing a variational model, and adaptively decomposes the gear vibration signal $x(t)$ by searching for the constrained variational optimal solution. The signal is adaptively decomposed into K IMFs $x_K(t)$: Finally, the decomposed IMFs $x_K(t)$ is used to construct the squared $L2$ norm of the VMD algorithm is expressed as:

$$\min_{\{u_K\},\{\omega_K\}} \left\{ \sum_{K=1}^{7} \left\| \partial_t \left[(\delta(t) + \frac{j}{\pi t}) \times x_K(t) \right] e^{-j\omega_K t} \right\|_2^2 \right\}$$
$$s.t. \sum_{K=1}^{7} u_K = x(t) \tag{1}$$

where: ∂_t is the partial derivative of t, $x(t)$ is the original signal, ω_K is the bandwidth center frequency, and δ_t is the pulse signal. According to the GMPSO algorithm proposed in this paper, the parameter combination $[K, \alpha]$ in the VMD decomposition algorithm is optimized, and the parameter combination $[K, \alpha]$ obtained by optimizing the vibration signals of normal gear, gear with tooth wear, gear with tooth crack and gear with tooth break are $[7, 2570]$, $[7, 4140]$, $[7, 4929]$ and $[7, 4322]$ respectively.

The constrained variational problem in the formula is further solved, and the quadratic penalty factor α and *Lagrange* multiplication operator $\lambda(t)$ are introduced in consideration of the fact that the constraint becomes non-constraint. The quadratic penalty factor α guarantees the signal reconstruction accuracy in the noise environment, and the *Lagrange* multiplication operator $\lambda(t)$ keeps the constraint condition strict. The extended Lagrange is defined as Equation (2):

$$\begin{aligned} &L\left(\{x_K\}, \{\omega_K\}, \{\lambda\}\right) \\ &= \alpha \sum_{K=1}^{7} \left\| \partial_t \left[(\delta(t) + \frac{j}{\pi t}) \times x_K(t) \right] e^{-j\omega_K t} \right\|_2^2 \\ &\quad + \left\| x(t) - \sum_{K=1}^{7} x_K(t) \right\|_2^2 + \left\langle \lambda(t), x(t) - \sum_{K=1}^{7} x_K(t) \right\rangle \end{aligned} \tag{2}$$

To solve the optimal solution of Equation (5), the alternating direction multiplication operator algorithm is used. The specific implementation steps of the algorithm are as follows:

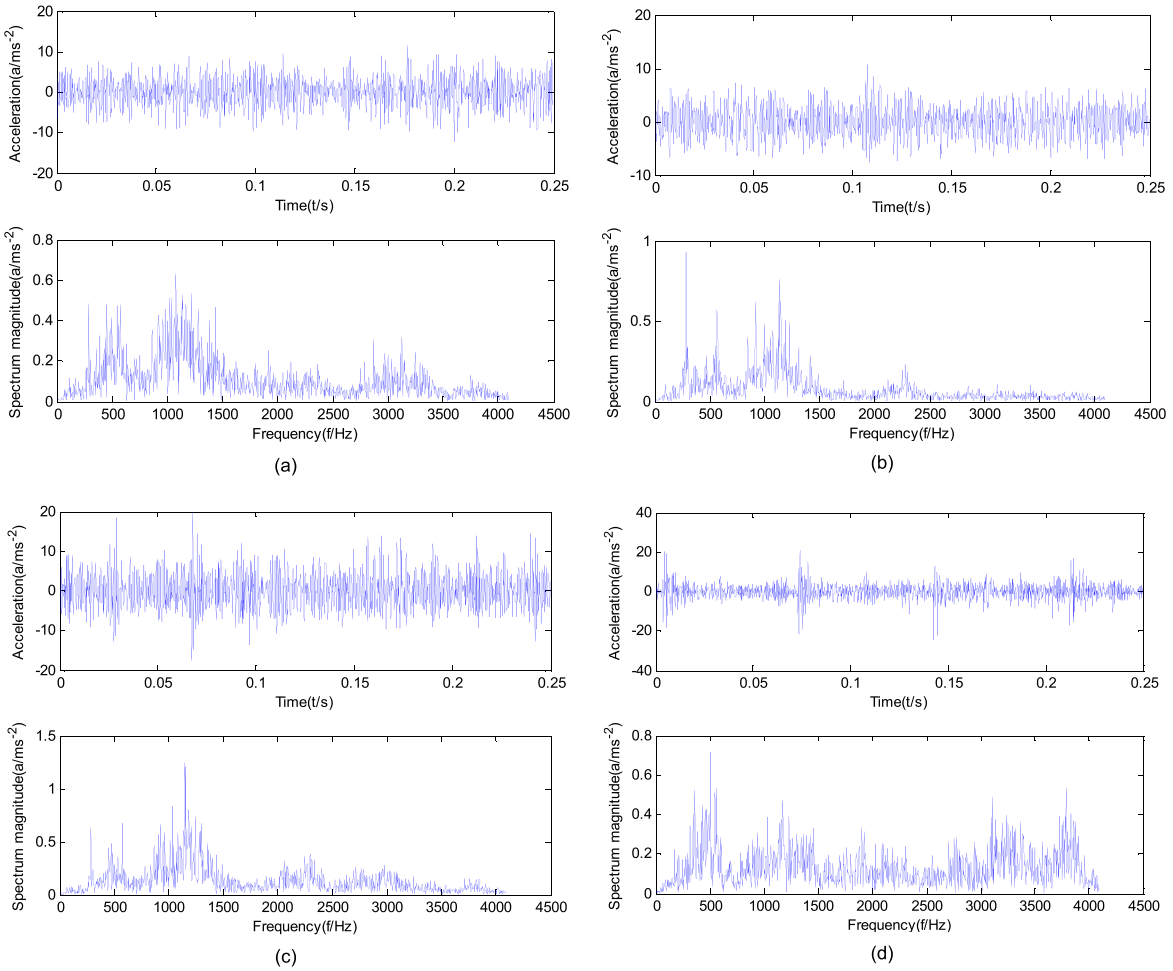

FIGURE 4. Time-domain and frequency-domain diagram of gear vibration signal: (a) Normal gear vibration signal, (b) gear with tooth wear vibration signal, (c) gear with tooth crack vibration signal, and (d) gear with tooth break vibration signal.

Firstly, initialize the parameters, including: $\{\hat{x}_K^1\}$, $\{\hat{\omega}_K^1\}$, $\{\hat{\lambda}_K^1\}$, mode function is 7, error ε, output $\{x_K\}$, $\{\omega_K\}$, λ.

Step 1. Execution loop $n = n + 1$;

Step 2. Update $\{\hat{x}_K\}$ for all $\omega \geq 0$;

$$\hat{x}_K^{n+1}(\omega) = \frac{\hat{x}(\omega) - \sum_{i \neq K} \hat{x}_i(\omega) + \hat{\lambda}_i(\omega)/2}{1 + 2\alpha(\omega - \omega_K)^2} \tag{3}$$

$$K \in [1, 10]$$

$$\alpha \in [0, 5000]$$

Step 3. Update the modal center frequency $\{\hat{\omega}_K\}$;

$$\hat{\omega}_K^{n+1} = \frac{\int_0^\infty \omega |u(\omega)|^2 d\omega}{\int_0^\infty |u_K(\omega)|^2 d\omega} \tag{4}$$

Step 4. Update λ;

$$\hat{\lambda}^{n+1}(\omega) = \hat{\lambda}^n(\omega) + \tau(\hat{x}(\omega) - \sum_{K=1}^{7} x_K^{n+1}(\omega)) \tag{5}$$

Step 5. Repeat steps 1-4 until the iteration stop condition is satisfied;

$$\sum_K \left\| \hat{x}_K^{n+1} - \hat{x}_K^n \right\|_2^2 \Big/ \left\| \hat{x}_K^n \right\|_2^2 < \varepsilon \tag{6}$$

Step 6. At the end of iteration, seven IMFs are obtained;

where: $x(t)$, $\hat{x}_i(\omega)$, $\hat{\lambda}(\omega)$ represents the Fourier transform of $\hat{x}(\omega)$, $x_i(\omega)$, $\lambda(\omega)$ respectively, and ε represents the discriminant accuracy.

The time-domain and frequency-domain diagrams of vibration signals collected under four working conditions of normal gear, gear with tooth wear, gear with tooth crack and gear with tooth break are shown in Figure 4.

From the above theoretical description, it can be seen that four parameters need to be determined in the VMD algorithm. They are the decomposition number K, penalty factor α, noise tolerance τ and the tolerance ε of the convergence criterion. Compared with parameters K and α, parameters τ and ε have less influence on the decomposition effect of VMD algorithm. In the actual VMD decomposition process, noise tolerance τ is usually 0, and the tolerance

ε of the convergence criterion is usually 10^{-7}. When the decomposition number K is small, the VMD algorithm will not be able to fully decompose the main frequency signal contained in the signal, that is, the under-decomposed state. When the decomposition number K is large, the VMD algorithm will decompose false components, that is, the over-decomposition state. Only when the decomposition number K is selected properly can the VMD algorithm decompose the signal into the main frequency components well. When the penalty factor α is too small, the VMD algorithm will also appear under-decomposed state. When the penalty factor α is too large, mode mixing will occur in the VMD algorithm.

To sum up, it can be seen that the choice of α and K will have a great impact on the decomposition effect of VMD algorithm, and the independent change of α and K will also affect the decomposition effect of VMD. Therefore, this paper adopts the parameter combination of $[K, \alpha]$ for overall optimization.

IV. PARAMETER ADAPTIVE OPTIMIZATION OF VMD METHOD BASED ON GMPSO

The previous section analyzed that different combinations of α and K would lead to different decomposition effects of VMD, that is, choosing combinations of α and K based on experience often fails to achieve the optimal decomposition effect of VMD. Therefore, swarm intelligence optimization algorithm is used to optimize the parameters of VMD. In this paper, GMPSO is used to optimize the parameter combination of α and K in the VMD algorithm until the optimal parameter combination of α and K is obtained.

A. GMPSO

Particle swarm optimization (PSO) as a swarm intelligence optimization algorithm, which has fast convergence speed and good global optimization ability. PSO algorithm is a swarm intelligence optimization algorithm proposed by Eberhart and Kennedy et al in 1995 [57], which is a global optimization algorithm. The PSO algorithm first generates and initializes a swarm of particles in a solution space. Each particle represents a potential optimal solution in the extremum optimization problem, and the three parameters of position, velocity and fitness value represent the characteristics of the particles. Among them, the fitness value is calculated by the fitness function, and its value represents the good or bad of the particle. PSO algorithm has the advantages of less input parameters and easy adjustment. However, it is also easy to fall into the local optimal and cannot obtain the global optimal approximate solution. Therefore, this paper utilize the idea of genetic algorithm mutation to construct genetic mutation particle swarm optimization (GMPSO) algorithm.

Define GMPSO algorithm: In a D-dimensional search space, the population of labeled particles is X, and the particle population X is composed of n particles, that is, the particle population $X = [x_1, x_2, \cdots, x_n]$, where the position of the $i-th$ particle in the search space is represented by a D-dimensional vector, that is, $x_i = [x_{i1}, x_{i2}, \cdots, x_{iD}]$, and the moving speed of the $i-th$ particle in the search space can also be represented by a D-dimensional vector, that is, $v_i = [v_{i1}, v_{i2}, \cdots, v_{iD}]$; Where, the local extreme value of the particle is $p_i = [p_{i1}, p_{i2}, \cdots, p_{iD}]$, the global extremum of the particle population is $G_1 = [g_1, g_2, \cdots, g_D]$, and the sub-global optimal value is $G_2 = [g'_1, g'_2, \cdots, g'_D]$. Among them, the maximum optimal iteration number of the particle individual is max Ita, and the mutation probability is q. In order to prevent individual particles trapped in local optimum, it is necessary to record the number of iterations in the process of particles in the iteration at any time, when the individual particles reach the optimal number of iterations wasn't up to the max Ita, each particle by updating the individual local extremum and particle population movement and the position of the global extremum to qualify for the next generation of particle population, update the Equation is:

$$\begin{aligned} v_i^{n+1} &= \omega v_i^n + c_1\eta\left(p_i - x_i^n\right) + c_2\eta\left(G_1 - x_i^n\right) \\ x_i^{n+1} &= x_i^n + x_i^{n+1} \end{aligned} \tag{7}$$

where, ω is the inertia weight, η is the random number between $[0, 1]$, c_1 and c_2 are the learning factors, which represent the local search ability and global search ability of the particle population respectively, and the number of iterations is n. Where, v_i, p_i, G_1, x_i are D dimensional vectors. The method to determine the inertia weight ω of the current iteration times is the linear decreasing weight method proposed by SHI, and the Equation is as follows:

$$\omega = \omega_{\max} - (\omega_{\max} - \omega_{\min})\, n/n_{\max} \tag{8}$$

where, $\omega_{\max}$ and $\omega_{\min}$ are the maximum and minimum inertia weights, n is the current iteration number, and $n_{\max}$ is the defined maximum iteration number. When the maximum optimal iteration number of the individual particle is max Ita, genetic mutation operation is used to update the particle position and moving speed to make it jump out of the local optimal.

B. ENVELOPE ENTROPY

As for the selection of fitness function in the GMPSO algorithm, Sun *et al.* [58] proposed the concept of envelope entropy E_p, which can be used as the standard for the optimization effect of PSO when optimizing VMD parameters. The basic concept is: the envelope entropy of time signal $x(j)$ with length N is defined as:

$$p_j = = a(j) / \sum_{j=1}^{N} a(j) \tag{9}$$

$$E_p = -\sum_{j=1}^{N} p_j \lg p_j \tag{10}$$

where, $j = 1, 2, \cdots, N$, $a(j)$ is the enveloping signal obtained by time signal $x(j)$ after Hilbert demodulation, and p_j is the result of normalization of enveloping signal $a(j)$.

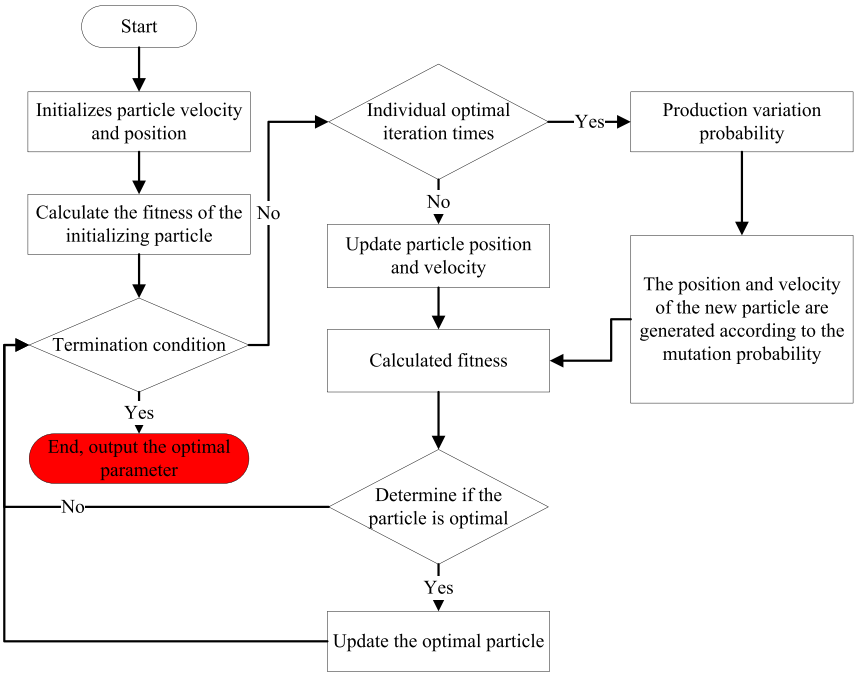

FIGURE 5. The flow chart of genetic mutation particle swarm optimization (GMPSO).

Among them, normalization can avoid the influence of different envelope amplitudes of IMFs components and reduce the interference of weak noises.

The early fault signal of the gear was decomposed by the VMD algorithm to obtain a number of IMFs, and then the envelope entropy value of each IMFs component was calculated separately. The larger the envelope entropy value, the more noise the IMFs component contained, and the less sparse the signal of the component. If the obtained IMFs component contains more fault-related periodic impact characteristic signals, the higher the sparsity of the obtained component signals, the lower the envelope entropy value.

When the $i-th$ particle is at a certain position x_i and moves at a certain velocity v_i (corresponding to a set of influence parameter combinations α and K), the calculation of the position under the condition of the gear fault signal after decomposition of VMD to get all of the IMFs envelope entropy weight, called envelope entropy value in a minimum of minimum entropy, expressed with min E_p^{IMFs}, and minimal entropy value corresponding to the IMFs component is after decomposition of VMD to get all of the IMFs component contains rich fault feature information of the best component, however, the weight is only local optimal weight. In order to search for the global optimal component, that is, to separate the IMFs component with the richest feature information from the gear fault signal, the minimum entropy value is taken as the fitness function in the optimization process, and the minimum entropy value is taken as the ultimate optimization objective. The optimization steps of α and K in the VMD algorithm are as follows:

(1) The parameters of the GMPSO algorithm are initialized and the fitness function is determined;

(2) The particle population is initialized, the parameter combination $[K, \alpha]$ in the VMD algorithm is taken as the position of the particle, a certain number of influencing parameter combinations are randomly generated as the initial position of the particle, and the moving velocity of each particle is randomly initialized;

(3) VMD was performed on the signal at different particle positions to calculate the fitness value min E_p^{IMFs} corresponding to each particle position;

(4) The fitness values were compared and the local extremum of the individual and the global extremum of the population were updated.

(5) When the number of iterations when the particle gets the local extreme value does not reach max *Ita*, the mutation probability q causes the particle to generate new position and moving speed;

(6) Update the velocity and position of the particle using step (4);

(7) Loop iteration, turn to step (3), and output the optimal fitness value and particle position after the iteration times reach the maximum set value.

C. PROPOSED METHOD

The GMPSO-VMD algorithm proposed in this paper takes the minimum envelope entropy value as the objective function, and achieves the optimization of the parameter combination $[K, \alpha]$ in the VMD algorithm through GMPSO.

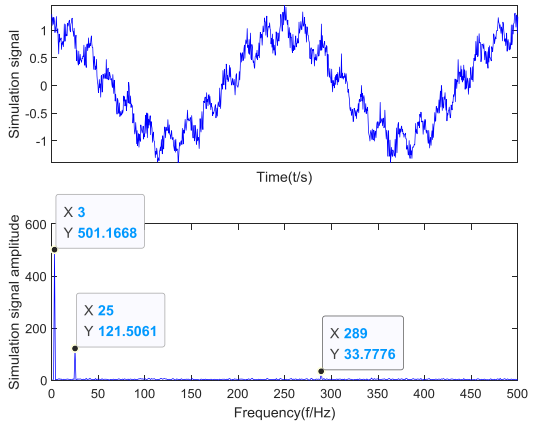

FIGURE 6. Time-domain and frequency-domain diagram of the simulation signal.

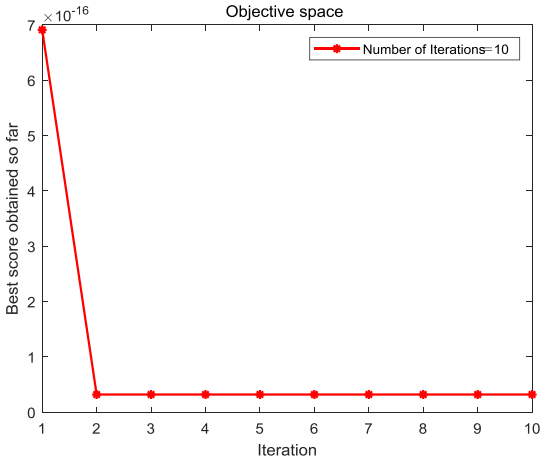

FIGURE 7. The GMPSO convergence curve of the simulation signal for VMD parameter optimization.

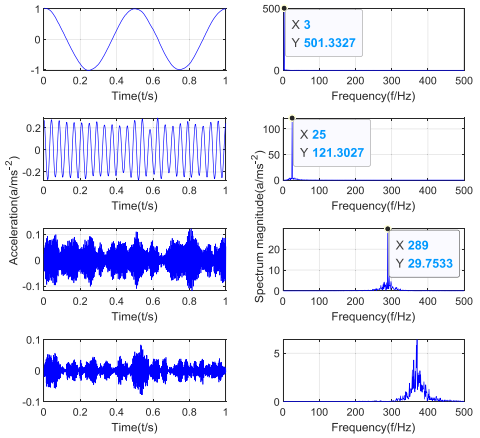

FIGURE 8. GMPSO-VMD decomposes the simulation signal.

The optimal combination is shown in formula 11. Since the original PSO algorithm is an optimization algorithm to obtain the minimum value, here the GMPSO algorithm makes the particle break away from the local minimum value with the variation probability q to achieve the global minimum envelop entropy value.

$$\begin{cases} fitness = \min\limits_{\beta=[K,\alpha]} \left\{E_p^{IMFs}\right\} \\ \quad s.t.\ K = [1, 10] \\ \alpha = [0, 5000] \end{cases} \tag{11}$$

where, fitness represents the objective function, E_p^{IMFs} is the envelope entropy of IMFs, $\beta = [K, \alpha]$ is the parameter set of the VMD to be optimized. In this study, K takes an integer in the intrval of $[1, 10]$, and α is assigned in the intrval of $[0, 5000]$.

In order to verify the effectiveness of the algorithm proposed in this paper, firstly, GMPSO-VMD algorithm is decomposed by using the simulation signal, and the simulation signal [35] is shown as follows:

$$\begin{cases} x_1(t) = \cos(2\pi\omega_1 t) \\ x_2(t) = \dfrac{\cos(2\pi\omega_2 t)}{4} \\ x_3(t) = \dfrac{\cos(2\pi\omega_3 t)}{16} \\ n(t) = \text{Gaussian white noise} \\ x(t) = x_1(t) + x_2(t) + x_3(t) + n(t) \end{cases} \tag{12}$$

where, $\omega_1, \omega_2, \omega_3$ are the frequencies of each component signal, and their values are $\omega_1 = 3$, $\omega_2 = 25$, $\omega_3 = 289$, t is time, $x_1(t), x_2(t), x_3(t)$ is fault signal, and $n(t)$ is Gaussian white noise. Figure 6 is the time-domain and frequency-domain diagram of the simulation signal $x(t)$.

Firstly, GMPSO is used to optimize the parameter combination $[K, \alpha]$ in the VMD algorithm. In the GMPSO algorithm, the fitness function is the minimum envelope entropy value of the simulation signal, and Figure 7 is the change curve of the minimum envelope entropy value of the simulation signal, which is a convergence curve and stable when the number of iterations increases. After GMPSO optimization, the optimal parameter combination of $[K, \alpha]$ is obtained as $[4, 4179]$.

After the VMD is optimized by GMPSO algorithm, the optimal combination of $[K, \alpha]$ obtained for the simulation signal is $[4, 4179]$. The optimal combination $[4, 4179]$ of $[K, \alpha]$ is put into the VMD algorithm, and then the optimized VMD algorithm is used to decompose the simulation signal into GMPSO-VMD. The GMPSO-VMD decomposition result is shown in Figure 8. Then EMD algorithm is used to decompose the simulation signal, so that the advantages of GMPSO-VMD algorithm and EMD algorithm can be compared. The simulation signal is decomposed by EMD algorithm, as shown in Figure 9.

As shown in Figure 8, the simulation signal is decomposed by GMPSO-VMD algorithm. It can be seen from the decomposition effect that the main frequency components such as $\omega_1 = 3$, $\omega_2 = 25$ and $\omega_3 = 289$ are all decomposed accurately. Therefore, the effectiveness of GMPSO-VMD algorithm can be obtained. As shown in Figure 9, its IMF1, IMF4 and IMF5 decomposed the main frequency components

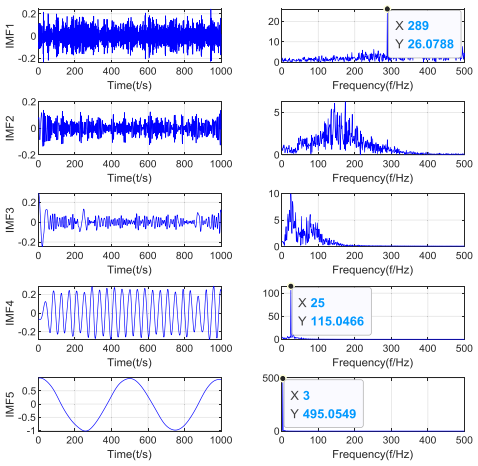

FIGURE 9. EMD decomposes the simulation signal.

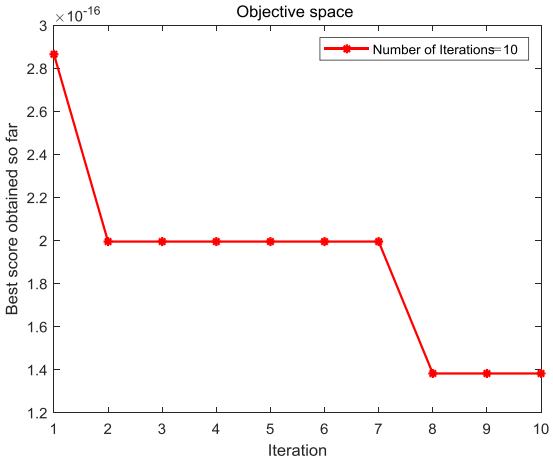

FIGURE 10. The GMPSO convergence curve of normal gear vibration signal for VMD parameter optimization.

such as $\omega_1 = 3$, $\omega_2 = 25$ and $\omega_3 = 289$, but IMF3 and IMF4 had mode mixing, and IMF4 frequency components existed in IMF3. It can be concluded that the GMPSO-VMD algorithm proposed in this paper can effectively overcome the mode mixing phenomenon in EMD algorithm.

Verify the validity of the proposed GMPSO-VMD algorithm, then the normal gear, gear with tooth wear, gear with tooth crack and gear with tooth break four types of gear fault signal GMPSO-VMD decomposition. Figure 10 shows the GMPSO convergence curve of normal gear vibration signal for VMD parameter optimization, Figure 11 shows the GMPSO convergence curve of gear with tooth wear vibration signal for VMD parameter optimization, Figure 12 shows the GMPSO convergence curve of gear with tooth crack vibration signal for VMD parameter optimization, Figure 13 shows the GMPSO convergence curve of gear with tooth break vibration signal for VMD parameter optimization.

After GMPSO optimization, the optimal combinations of $[K, \alpha]$ in the VMD algorithm are $[7, 2570]$, $[7, 4140]$, $[7, 4929]$ and $[7, 4322]$. Then, the optimized $[K, \alpha]$ optimal

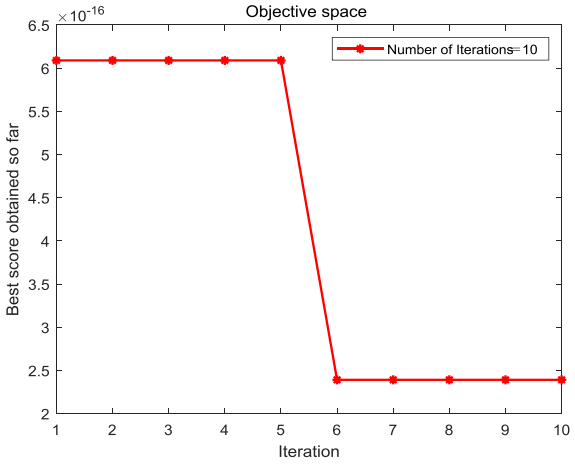

FIGURE 11. The GMPSO convergence curve of gear with tooth wear vibration signal for VMD parameter optimization.

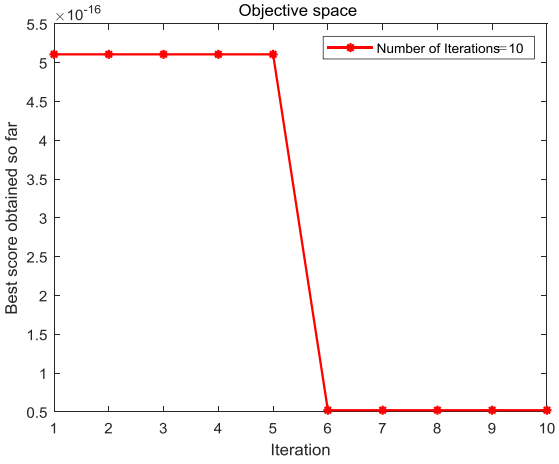

FIGURE 12. The GMPSO convergence curve of gear with tooth crack vibration signal for VMD parameter optimization.

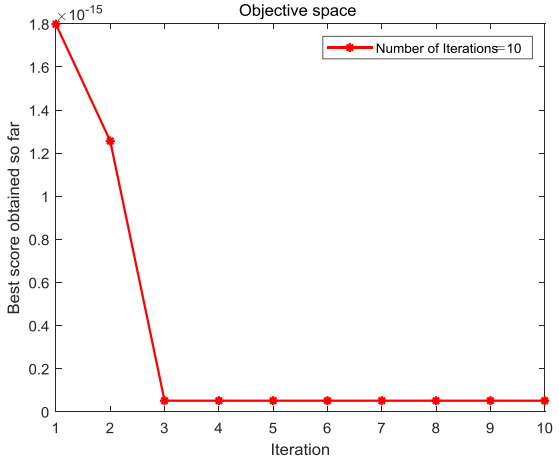

FIGURE 13. The GMPSO convergence curve of gear with tooth break vibration signal for VMD parameter optimization.

parameter combination was put into GMPSO-VMD algorithm, and then the GMPSO-VMD algorithm was used to decompose the vibration signals of normal gear, gear with tooth wear, gear with tooth crack and gear with tooth break.

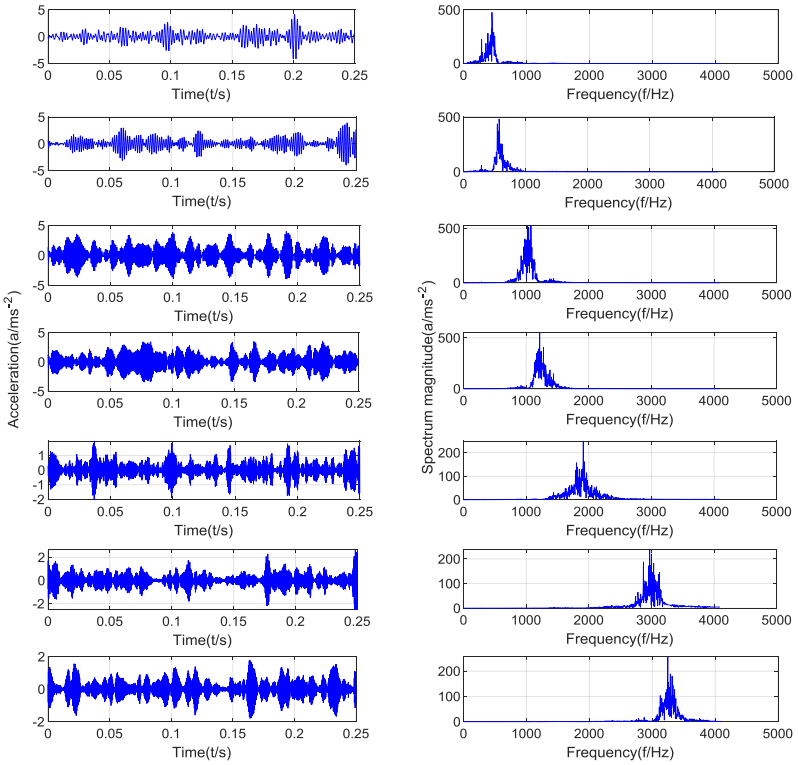

FIGURE 14. Normal gear vibration signal GMPSO-VMD decomposition time-domain waveform and spectrum.

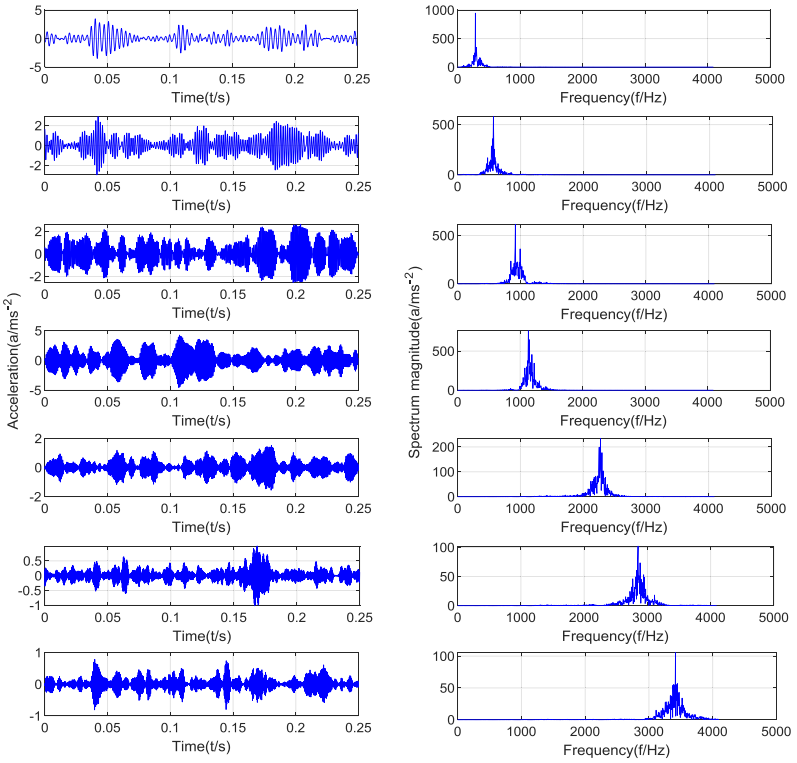

FIGURE 15. Gear with tooth wear vibration signal GMPSO-VMD decomposition time-domain waveform and spectrum.

Figure 14 shows the time-domain waveform and spectrum of normal gear vibration signal decomposed by GMPSO-VMD algorithm. Figure 15 shows the time-domain waveform and spectrum of gear with tooth wear vibration signal

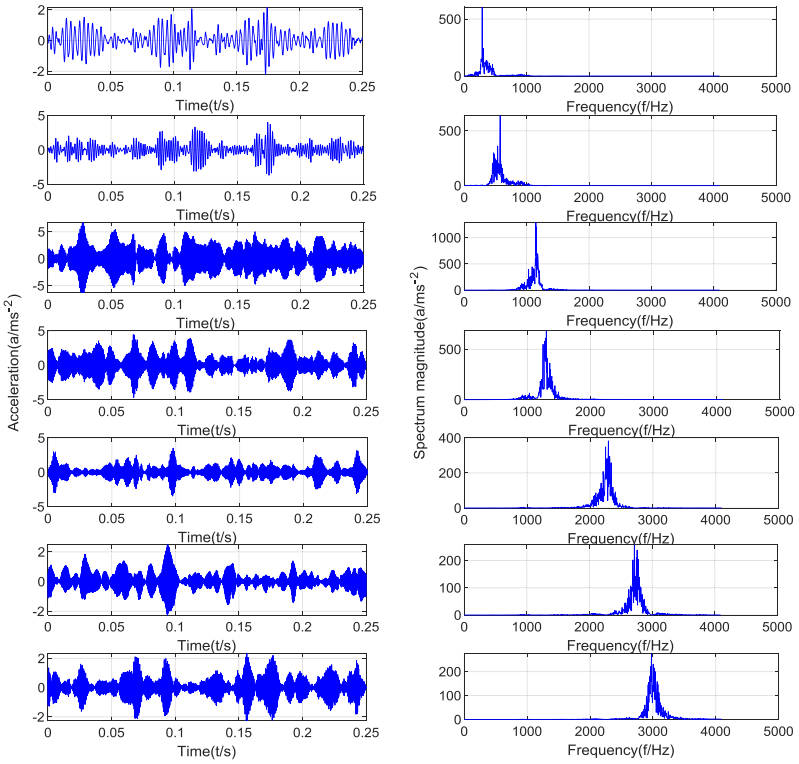

FIGURE 16. Gear with tooth crack vibration signal GMPSO-VMD decomposition time-domain waveform and spectrum.

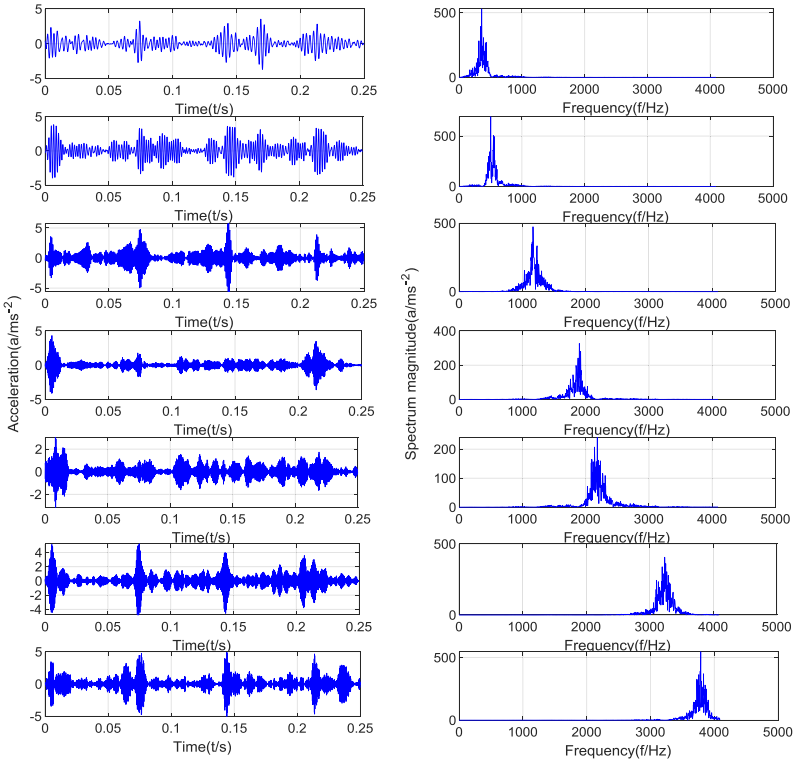

FIGURE 17. Gear with tooth break vibration signal GMPSO-VMD decomposition time-domain waveform and spectrum.

decomposed by GMPSO-VMD algorithm. Figure 16 shows the time-domain waveform and spectrum of gear with tooth crack vibration signal decomposed by GMPSO-VMD algorithm. Figure 17 shows the time-domain waveform and

TABLE 1. Sample entropy values of each intrinsic mode functions (IMFs).

Gear Fault Type	Sample Number	SE1	SE2	SE3	SE4	SE5	SE6	SE7
Normal gear	1	0.66	0.63	0.69	0.74	1.07	0.79	0.75
	2	0.66	0.66	0.66	0.69	0.99	0.72	0.67
	3	0.67	0.71	0.68	0.73	0.93	0.73	0.71
	4	0.66	0.64	0.64	0.70	0.99	0.67	0.67
Gear with tooth wear	1	0.59	0.63	0.63	0.54	0.68	0.78	0.72
	2	0.60	0.65	0.65	0.53	0.67	0.82	0.72
	3	0.62	0.65	0.65	0.54	0.65	0.70	0.69
	4	0.61	0.63	0.65	0.54	0.57	0.88	0.68
Gear with tooth crack	1	0.62	0.65	0.54	0.57	0.60	0.66	0.60
	2	0.66	0.64	0.57	0.56	0.66	0.73	0.64
	3	0.62	0.65	0.64	0.59	0.67	0.61	0.58
	4	0.69	0.65	0.64	0.53	0.62	0.60	0.65
Gear with tooth break	1	0.61	0.62	0.64	0.67	0.68	0.65	0.63
	2	0.65	0.63	0.67	0.73	0.67	0.65	0.69
	3	0.65	0.62	0.61	0.66	0.83	0.68	0.65
	4	0.64	0.58	0.59	0.64	0.72	0.66	0.63

spectrum of gear with tooth break vibration signal decomposed by GMPSO-VMD algorithm.

D. SAMPLE ENTROPY

Sample Entropy is a new measure of time series complexity proposed by Richman and Moornan [59]. From the perspective of time series complexity, sample entropy measures the probability of the system generating new patterns, and quantitatively describes the complexity and regularity of the system. Sample entropy is calculated as the logarithm of sum, aiming to reduce the error of approximate entropy, which is more closely consistent with the known random part. Sample entropy is a better method similar to the current approximate entropy with single precision. The calculation steps of sample entropy are as follows:

Step 1. The decomposed IMFs $\{x_K(t)\,|1 \le t \le N\}$ is given the mode dimension, and the original sequence is used to form $\{x_K(t)\,|1 \le t \le N\}$ group of m-dimension vectors $x_K(t)$:

$$x_K(t) = (x_K(t), x_K(t+1), \cdots, x_K(t+m-1)) \quad (13)$$

where: $t = 1, 2, \cdots, N-m+1$, $x_K(t)$ is the IMFs of the original gear vibration signal decomposed by GMPSO-VMD.

Step 2. The maximum distance between two m-dimensional vectors $x(T)$ and $x(t)$ is defined as formula 8:

$$d(T,t) = \max_{K=0,1,\cdots,m-1} |x(T+K) - x(t+K)| \quad (14)$$

Step 3. For a given threshold r, the number H of distances $d(i,j)$ less than r is counted and divided by the total number of distances $N-m+1$, denoted $B_i^m(r)$.

$$B_i^m(r) = \frac{H}{N-m+1} \quad (15)$$

where: $1 \le T \le N-m+1$, $1 \le t \le N-m+1$, $i \ne j$

The average value is defined as:

$$B^m(r) = \frac{1}{N-m+1} \sum_{i=1}^{N-m+1} B_i^m(r) \quad (16)$$

Step 4. For $m+1$, repeat steps 1-3 to get $B^{m+1}(r)$.

Step 5. For a given threshold r, the sample entropy of the subsequence is defined as:

$$SampEn(m,r) = \lim_{N\to\infty} \left[-\ln \frac{B^{m+1}(r)}{B^m(r)} \right] \quad (17)$$

When N is a finite value of the sequence length, the estimated value of sample entropy of the time series is:

$$SampEn(m,r,N) = -\ln \frac{B^{m+1}(r)}{B^m(r)} \quad (18)$$

Compared with the approximate entropy, the sample entropy has the following characteristics: First, the sample entropy does not include the comparison of its own data segment, which is the exact value of the negative mean natural logarithm of the conditional probability, so the calculation of the sample entropy does not depend on the data length. Second, sample entropy has better consistency.

In this paper, GMPSO optimization algorithm is used to optimize the VMD algorithm, and gear fault vibration signal is decomposed by GMPSO-VMD algorithm, and the decomposition number is 7. The original gear fault vibration signal is decomposed into 7 IMFs. The feature information of each gear fault is included in IMFs. In this paper, the sample entropy value of each IMFs is extracted as its feature vector and input into the subsequent fault diagnosis model for fault identification.

The 16 groups of gear vibration signal collected under 4 states were decomposed into GMPSO-VMD, the 7 IMFs components decomposed by GMPSO-VMD were selected to extract sample entropy value. SE1 represent the sample entropy value of IMF1, SE2 represent the sample entropy value of IMF2, SE3 represent the sample entropy value of IMF3, SE4 represent the sample entropy value of IMF4, SE5 represent the sample entropy value of IMF5, SE6 represent the sample entropy value of IMF6, and SE7 represent the sample entropy value of IMF7. The sample entropy value matrix of each component is shown in Table1.

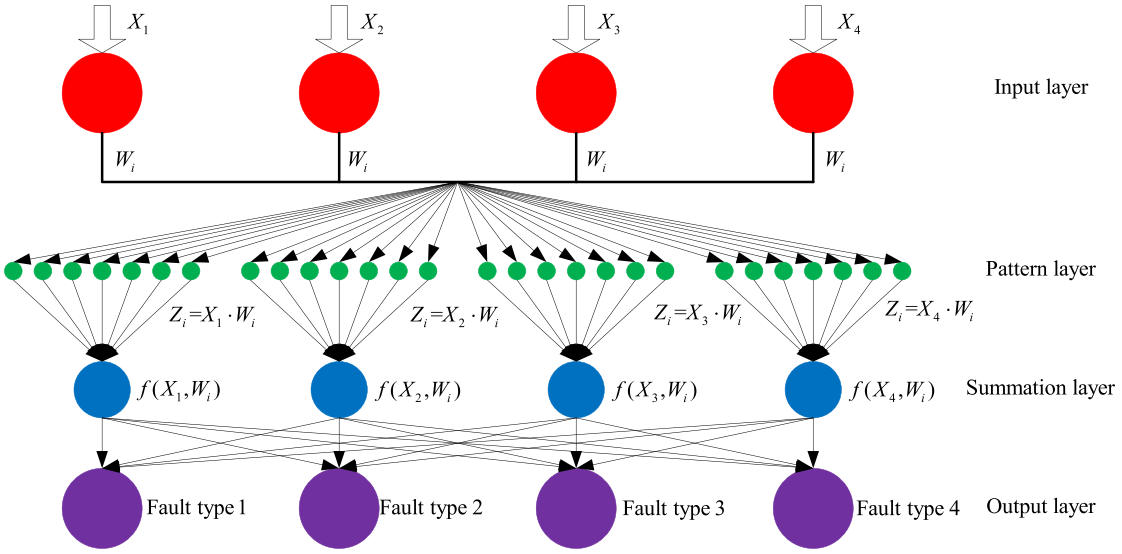

FIGURE 18. Probabilistic neural network (PNN) structure in this paper.

V. PROBABILISTIC NEURAL NETWORK FAULT DIAGNOSIS MODEL

A. PNN STRUCTURE

Probabilistic neural network (PNN) was first proposed by D. F. Spaiht in 1989 [54]. It is a parallel algorithm developed based on Bayes classification rules and Parzen window's probability density function estimation method. PNN is a supervised learning neural network and is widely used in pattern recognition and fault diagnosis. In the practical application, especially in the application of fault diagnosis, the advantage of PNN lies in the use of linear learning algorithm to complete the work done by the nonlinear learning algorithm, at the same time, it also maintains the high precision of the nonlinear algorithm and other characteristics.

PNN is a feedforward neural network developed from radial basis function network. Its theoretical basis is Bayesian minimum risk criterion (namely Bayesian decision theory). PNN as a kind of radial basis network, is widely used in pattern classification. The basic structure of PNN is shown in Figure 18. It is composed of four layers: input layer, pattern layer, summation layer and output layer. The corresponding weight of PNN is the distribution of sample data, and the network can satisfy the real-time data processing in training without training.

B. PNN ALGORITHM

(1) The input layer receives the feature vectors from the training samples, and then transmits the feature vectors to PNN. The number of neurons in the input layer is equal to the dimension of the training sample feature vectors X. Each neuron constitutes the feature vectors X and the weight vectors W_i, where $Z_i = X \cdot W_i$ is the input to the pattern layer.

(2) The pattern layer calculates the matching relationship between the input feature vector and each mode in the training samples. The number of neurons in the pattern layer is equal to the sum of the training samples of each fault category. The output of each mode unit in this layer is:

$$f(X, W_i) = \exp\left[-\frac{(X - W_i)^T (X - W_i)}{2\delta^2}\right] \tag{19}$$

where, W_i is the weight of the connection between the input layer and the pattern layer, δ is the smoothing factor, and X is the input feature vectors.

(3) The third layer is the summation layer, which accumulates the probabilities originally belonging to a certain class and calculates the probability value according to the above formula, so as to obtain the estimated probability density function of the fault category. Among them, each fault category has only one summation layer neuron, which is connected to the mode layer neuron belonging to its own fault category, but not to the neurons of other fault categories in the mode layer. Therefore, the sum layer neuron simply adds up the output of the pattern layer neuron belonging to its own fault category, independent of the output of other fault categories in the pattern layer. The output of neurons in the summation layer is proportional to the estimation of the probability density of each fault category. Through the normalization of the output layer, the probability estimation of each fault category can be obtained as follows:

$$P(X|W_i) = \frac{1}{(2\pi)^{\frac{n}{2}}\delta^n N_i}\sum_{j=1}^{N_i}\exp\frac{-(X-X_{ij})^T(X-X_{ij})}{2\delta^2} \tag{20}$$

where, X_{ij} is the column sample of W_i, n is the dimension of the sample feature vectors, and N_i is the sum of samples of W_i.

(4) The output layer of PNN consists of a simple threshold discriminator, whose function is to select a neuron with the maximum posterior probability density from the estimated

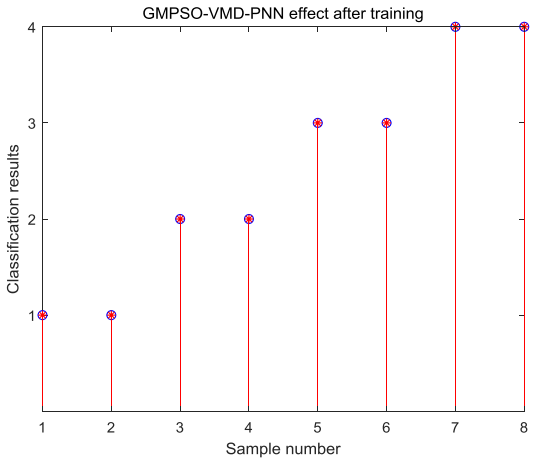

FIGURE 19. GMPSO-VMD-PNN gear fault training identification result.

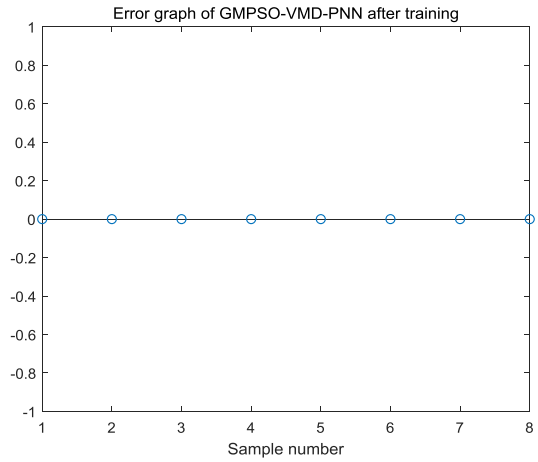

FIGURE 20. GMPSO-VMD-PNN gear fault training error.

probability density of each fault category as the output of the whole system. Output layer neurons is a kind of competition neurons, each neuron respectively corresponding to a kind of fault category, number of output layer neurons is equal to the number of the kinds of the training sample data it receives from the summation output layer of various fault categories of probability density function, one of the biggest probability density function of the neuron output is 1, which corresponds to the type of unknown samples fault category, full of 0 to other neurons. Where, when the value of distribution density SPREAD is close to 0, it constitutes the nearest classifier. When the SPREAD value is large, it constitutes an adjacent classifier for several training samples.

VI. FAULT DIAGNOSIS AND RESULT ANALYSIS OF GMPSO-VMD-PNN

Two sets of data were randomly selected from the sample entropy values of four kinds of gear fault vibration signals in Table 1, including normal gear, gear with tooth wear, gear with tooth crack and gear with tooth break. A total of 8 sets of sample entropy values were obtained, which constituted the GMPSO-VMD-PNN training matrix. The sample entropy values of the remaining 8 groups constituted the GMPSO-VMD-PNN test matrix. Among them, the training matrix and the test matrix each contain two sets of sample entropy feature vectors of gear samples of normal gear, gear with tooth wear, gear with tooth crack and gear with tooth break.

Firstly, the training matrix is input into GMPSO-VMD-PNN to obtain the gear fault identification result and training error after training of GMPSO-VMD-PNN. Then the test matrix is input into the trained GMPSO-VMD-PNN, and the classification result of GMPSO-VMD-PNN on the vibration signal of gear fault is obtained. Figure 19 is the gear fault identification result after GMPSO-VMD-PNN training, Figure 20 is the training error after GMPSO-VMD-PNN training, and Figure 21 is the gear fault identification result of GMPSO-VMD-PNN.

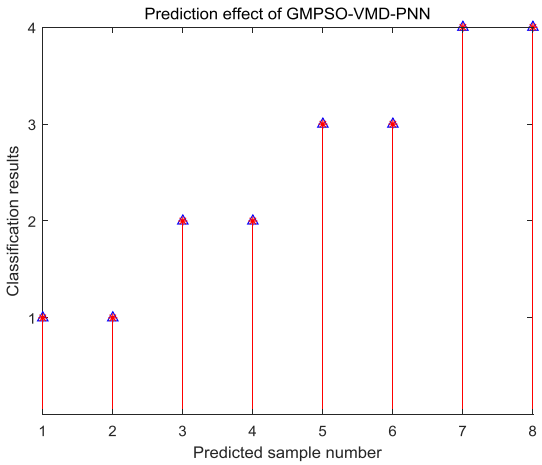

FIGURE 21. GMPSO-VMD-PNN gear fault diagnosis and identification results.

According to Figure 19 and Figure 20, the vibration signal training matrix of gear fault is trained by GMPSO-VMD-PNN. The training error is 0, the training accuracy is 100%, and the training accuracy is better.

According to Figure 21, the gear fault vibration signal test matrix was diagnosed by GMPSO-VMD-PNN, and each gear fault category was accurately classified, and the accuracy of gear fault diagnosis was 100%. The effectiveness of GMPSO-VMD-PNN algorithm in gear fault diagnosis is proved.

In order to verify the superiority of GMPSO-VMD-PNN algorithm proposed in this paper, the proposed algorithm is compared with VMD-PNN, EMD-PNN and CEEMDAN-PNN algorithm in the accuracy of gear fault diagnosis. Firstly, the training matrix is input into VMD-PNN to obtain the gear fault identification result and training error of VMD-PNN after training. Then the test matrix is input into the trained VMD-PNN, and the classification result of VMD-PNN on the vibration signal of gear fault is obtained.

Figure 22 is the gear fault identification result after VMD-PNN training, Figure 23 is the training error after

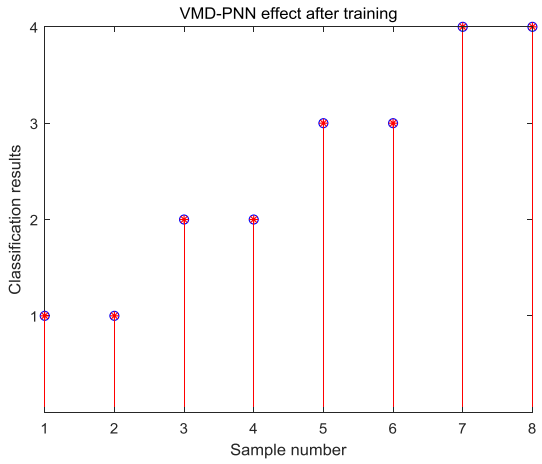

FIGURE 22. VMD-PNN gear fault training identification result.

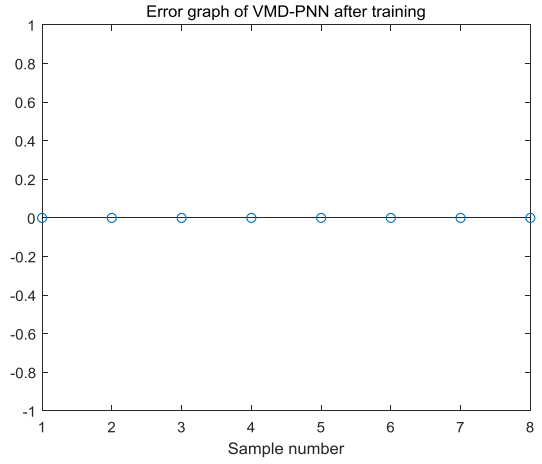

FIGURE 23. VMD-PNN gear fault training error.

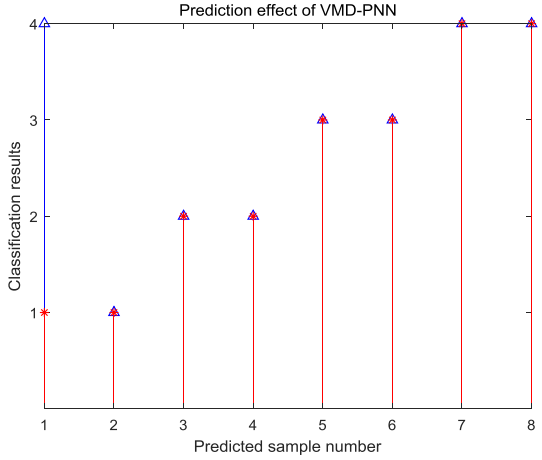

FIGURE 24. VMD-PNN gear fault diagnosis and identification results.

VMD-PNN training, and Figure 24 is the gear fault identification result of VMD-PNN.

According to Figure 22 and Figure 23, the vibration signal training matrix of gear fault is trained by VMD-PNN.

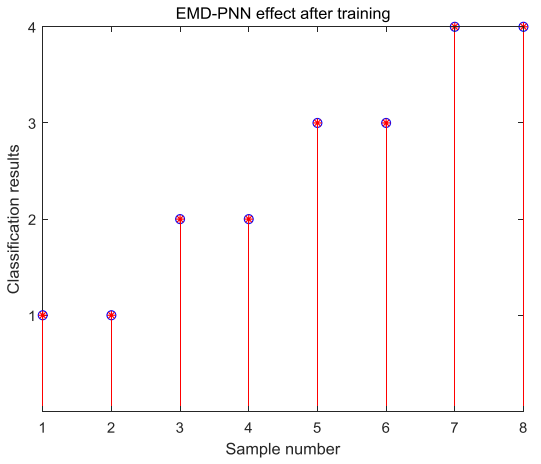

FIGURE 25. EMD-PNN gear fault training identification result.

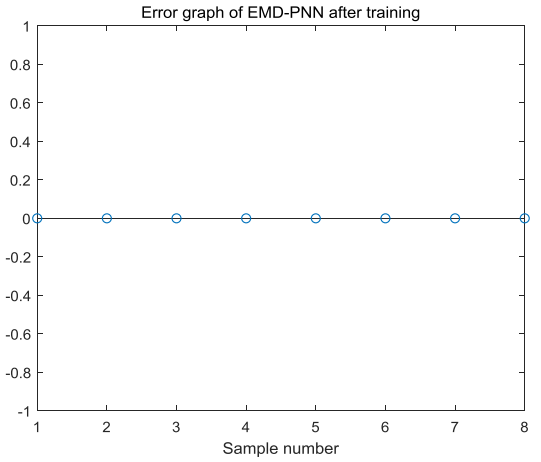

FIGURE 26. EMD-PNN gear fault training error.

The training error is 0, the training accuracy is 100%, and the training accuracy is better.

As shown in Figure 24, the test matrix of wheel fault vibration signal was diagnosed by VMD-PNN. In the normal gear vibration signal category, one group of signals was classified incorrectly, while the rest of each gear fault category was accurately classified, and the accuracy rate of gear fault diagnosis was 87.5%.

Then the accuracy of gear fault is compared with EMD-PNN algorithm. Firstly, the training matrix is input into EMD-PNN to obtain the gear fault identification result and training error of EMD-PNN after training. Then the test matrix is input into the trained EMD-PNN, and the classification result of EMD-PNN on the vibration signal of gear fault is obtained.

Figure 25 is the gear fault identification result after EMD-PNN training, Figure 26 is the training error after EMD-PNN training, and Figure 27 is the gear fault identification result of EMD-PNN.

According to Figure 25 and Figure 26, the vibration signal training matrix of gear fault is trained by EMD-PNN. The training error is 0, the training accuracy is 100%, and the training accuracy is better.

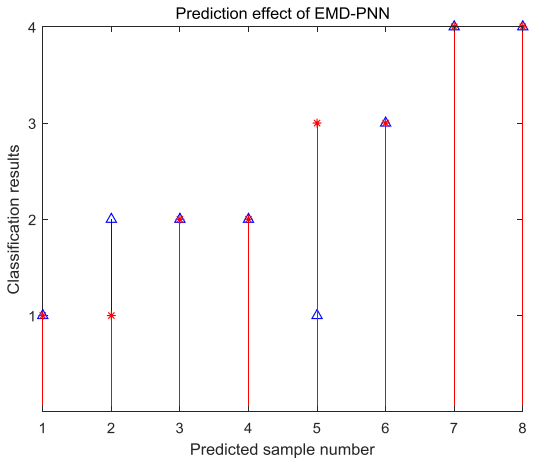

FIGURE 27. EMD-PNN gear fault diagnosis and identification results.

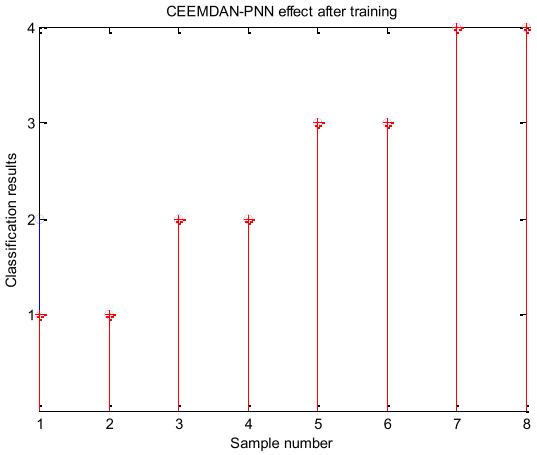

FIGURE 28. Complete ensemble empirical mode decomposition adaptive noise probabilistic neural network (CEEMDAN-PNN) gear fault training identification result.

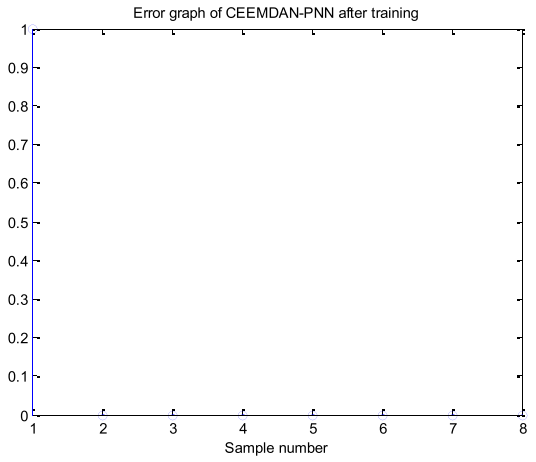

FIGURE 29. CEEMDAN-PNN gear fault training error.

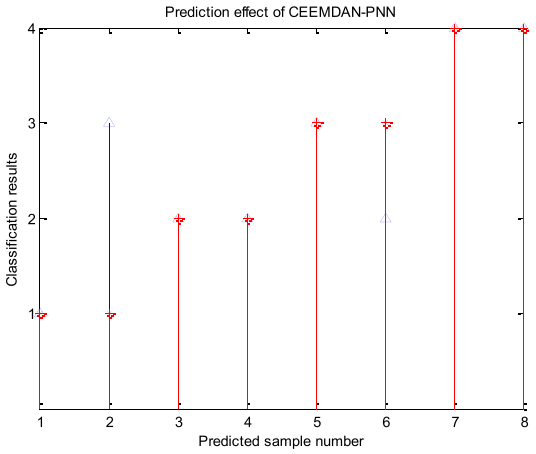

FIGURE 30. CEEMDAN-PNN gear fault diagnosis and identification results.

According to Figure 27, the gear fault vibration signal test matrix was diagnosed by EMD-PNN, and there was a group of classification errors in the normal gear vibration signal and gear with tooth crack vibration signal categories, while the rest of each gear fault category was accurately classified, with the accuracy rate of gear fault diagnosis was 75%.

Then the accuracy of gear fault is compared with CEEMDAN-PNN algorithm. Firstly, the training matrix is input into CEEMDAN-PNN to obtain the gear fault identification result and training error of CEEMDAN-PNN after training. Then the test matrix is input into the trained CEEMDAN-PNN, and the classification result of CEEMDAN-PNN on the vibration signal of gear fault is obtained.

Figure 28 is the gear fault identification result after CEEMDAN-PNN training, Figure 29 is the training error after CEEMDAN-PNN training, and Figure 30 is the gear fault identification result of CEEMDAN-PNN.

According to Figure 28 and Figure 29, the vibration signal training matrix of gear fault is trained by CEEMDAN-PNN. The training error is 12.5%, the training accuracy is 87.5%, and the training accuracy is better.

According to Figure 30, the gear fault vibration signal test matrix was diagnosed by CEEMDAN-PNN, and there was a group of classification errors in the normal gear vibration signal and gear with tooth crack vibration signal categories, while the rest of each gear fault category was accurately classified, with the accuracy rate of gear fault diagnosis was 75%. According to the comparison of accuracy of gear fault diagnosis above, GMPSO-VMD-PNN algorithm can improve the accuracy of gear fault diagnosis compared with VMD-PNN algorithm, EMD-PNN algorithm and CEEMDAN-PNN
algorithm.

According to different classification algorithms. In this paper, SVM algorithm is used to replace PNN algorithm for gear fault diagnosis. Table 2 shows the accuracy of gear fault diagnosis after each classification algorithm is matched with each other.

Among them, the training results represent the accuracy of the overall classification system of PNN after the training of gear fault data. When the training results are good,

TABLE 2. The accuracy of gear fault diagnosis by different decomposition algorithms and classification algorithms.

Decomposition Algorithm	Classification Algorithm	Fault Diagnosis Identification Rate
GMPSO-VMD	PNN	100%
VMD	PNN	87.5%
EMD	PNN	75%
CEEMDAN	PNN	75%
GMPSO-VMD	SVM	14.29%
VMD	SVM	14.29%
EMD	SVM	28.57%
CEEMDAN	SVM	0%

the classification effect reaches the standard. The test results represent the classification of gear fault data by PNN after training. The results only represent the accuracy of gear data, not the PNN system after training.

According to the comparison between Figure 8 and Figure 9, the GMPSO-VMD proposed in this paper can effectively avoid the disadvantages such as mode mixing in EMD algorithm, and has a certain influence on improving the accuracy of gear fault diagnosis. In according to the different decomposition algorithm in Table 2 with different classification algorithm combined with the comparative results of gear fault diagnosis accuracy, the proposed GMPSO-VMD-PNN algorithm in terms of gear fault diagnosis accuracy is 100%, other algorithms in terms of gear fault diagnosis on mean there is a certain error, especially the SVM classification algorithm in terms of gear fault diagnosis accuracy rate is very low. Therefore, the GMPSO-VMD-PNN algorithm proposed in this paper has certain application prospects in gear fault diagnosis.

VII. CONCLUSION

In this paper, a gear fault diagnosis based on GMPSO-VMD-PNN algorithm is proposed, and the following conclusions are obtained:

(1) GMPSO-VMD algorithm can effectively avoid the adverse effects of mode confusion in EMD algorithm, and overcome the difficulty of parameter selection in VMD algorithm. GMPSO-VMD algorithm can adaptively obtain the optimal parameter combination $[K, \alpha]$ of signals to be analyzed. Moreover, the sample entropy of samples is selected as the signal feature vectors, which can not only retain the effective fault information in the signal, but also effectively eliminate the interference of noise.

(2) In GMPSO-VMD algorithm, the minimum envelope entropy value is selected as the fitness function of GMSPO algorithm, and the optimal parameter combination of $[K, \alpha]$ in the VMD algorithm can be quickly and effectively found. In addition, in the GMPSO-VMD algorithm, the mutation probability q is used to generate new positions and moving velocities of particles, which can effectively avoid the generation of local minima.

(3) The effectiveness and feasibility of the GMPSO-VMD-PNN algorithm proposed in this paper are verified by taking four kinds of vibration signal fault diagnosis of gear faults as examples. By comparing with fixed parameter VMD algorithm, EMD algorithm and CEEMDAN-PNN algorithm, the superiority of GMPSO-VMD-PNN in gear fault vibration signal analysis and fault feature extraction is verified. Therefore, this study has certain potential value for gear fault diagnosis. The method proposed in this paper can be applied to the fault diagnosis of other mechanical parts, such as bearings and other rotating mechanical parts.

REFERENCES

[1] X. Liang, M. J. Zuo, and Z. Feng, "Dynamic modeling of gearbox faults: A review," *Mech. Syst. Signal Process.*, vol. 98, pp. 852–876, Jan. 2018.
[2] M. C. Garcia, M. A. Sanz-Bobi, and J. Del Pico, "SIMAP: Intelligent system for predictive maintenance: Application to the health condition monitoring of a windturbine gearbox," *Comput. Ind.*, vol. 57, no. 6, pp. 552–568, 2006.
[3] A. Ragheb and M. Ragheb, "Wind turbine gearbox technologies," in *Proc. 1st Int. Nucl. Renew. Energy Conf. (INREC)*, Mar. 2010, pp. 1–8.
[4] S. Wei, J. Zhao, Q. Han, and F. Chu, "Dynamic response analysis on torsional vibrations of wind turbine geared transmission system with uncertainty," *Renew. Energy*, vol. 78, pp. 60–67, Jun. 2015.
[5] J. P. Salameh, S. Cauet, E. Etien, A. Sakout, and L. Rambault, "Gearbox condition monitoring in wind turbines: A review," *Mech. Syst. Signal Process.*, vol. 111, pp. 251–264, Oct. 2018.
[6] D. Xiao, J. Ding, X. Li, and L. Huang, "Gear fault diagnosis based on kurtosis criterion VMD and SOM neural network," *Appl. Sci.*, vol. 9, no. 24, p. 5424, Dec. 2019.
[7] B. Merainani, D. Benazzouz, and C. Rahmoune, "Early detection of tooth crack damage in gearbox using empirical wavelet transform combined by Hilbert transform," *J. Vib. Control*, vol. 23, no. 10, pp. 1623–1634, Jun. 2017.
[8] T. Bruce, E. Rounding, H. Long, and R. Dwyer-Joyce, "Characterisation of white etching crack damage in wind turbine gearbox bearings," *Wear*, vols. 338–339, pp. 164–177, Sep. 2015.
[9] Y. Lei, D. Han, J. Lin, and Z. He, "Planetary gearbox fault diagnosis using an adaptive stochastic resonance method," *Mech. Syst. Signal Process.*, vol. 38, no. 1, pp. 113–124, Jul. 2013.
[10] X. Liang, M. J. Zuo, and M. R. Hoseini, "Vibration signal modeling of a planetary gear set for tooth crack detection," *Eng. Failure Anal.*, vol. 48, pp. 185–200, Feb. 2015.
[11] Z. Zeng, K. Ding, G. He, and W. Li, "Space-time model and spectrum mechanism on vibration signal for planetary gear drive," *Mech. Syst. Signal Process.*, vol. 129, pp. 164–185, Aug. 2019.
[12] Y. Guo, L. Zhao, X. Wu, and J. Na, "Vibration separation technique based localized tooth fault detection of planetary gear sets: A tutorial," *Mech. Syst. Signal Process.*, vol. 129, pp. 130–147, Aug. 2019.
[13] N. Barbieri, G. De Sant'anna Vitor Barbieri, B. M. Martins, L. De Sant'anna Vitor Barbieri, and K. F. De Lima, "Analysis of automotive gearbox faults using vibration signal," *Mech. Syst. Signal Process.*, vol. 129, pp. 148–163, Aug. 2019.
[14] M. Soualhi, K. T. Nguyen, A. Soualhi, K. Medjaher, and K. E. Hemsas, "Health monitoring of bearing and gear faults by using a new health indicator extracted from current signals," *Measurement*, vol. 141, pp. 37–51, Jul. 2019.
[15] D. F. Plöger, P. Zech, and S. Rinderknecht, "Vibration signature analysis of commodity planetary gearboxes," *Mech. Syst. Signal Process.*, vol. 119, pp. 255–265, Mar. 2019.
[16] S. Schmidt and P. S. Heyns, "An open set recognition methodology utilising discrepancy analysis for gear diagnostics under varying operating conditions," *Mech. Syst. Signal Process.*, vol. 119, pp. 1–22, Mar. 2019.
[17] X. Li, J. Li, Y. Qu, and D. He, "Gear pitting fault diagnosis using integrated CNN and GRU network with both vibration and acoustic emission signals," *Appl. Sci.*, vol. 9, no. 4, p. 768, Feb. 2019.
[18] Y. Qu, D. He, J. Yoon, B. Van Hecke, E. Bechhoefer, and J. Zhu, "Gearbox tooth cut fault diagnostics using acoustic emission and vibration sensors—A comparative study," *Sensors*, vol. 14, no. 1, pp. 1372–1393, Jan. 2014.
[19] N. Baydar and A. Ball, "Detection of gear failures via vibration and acoustic signals using wavelet transform," *Mech. Syst. Signal Process.*, vol. 17, no. 4, pp. 787–804, Jul. 2003.

[20] N. Baydar and A. Ball, "A comparative study of acoustic and vibration signals in detection of gear failures using Wigner–Ville distribution," *Mech. Syst. Signal Process.*, vol. 15, no. 6, pp. 1091–1107, Nov. 2001.

[21] H. Zheng, Z. Li, and X. Chen, "Gear fault diagnosis based on continuous wavelet transform," *Mech. Syst. Signal Process.*, vol. 16, nos. 2–3, pp. 447–457, Mar. 2002.

[22] J. Rafiee, M. Rafiee, and P. Tse, "Application of mother wavelet functions for automatic gear and bearing fault diagnosis," *Expert Syst. Appl.*, vol. 37, no. 6, pp. 4568–4579, Jun. 2010.

[23] G. Cheng, Y.-L. Cheng, L.-H. Shen, J.-B. Qiu, and S. Zhang, "Gear fault identification based on Hilbert–Huang transform and SOM neural network," *Measurement*, vol. 46, no. 3, pp. 1137–1146, Apr. 2013.

[24] X. Yu, E. Ding, C. Chen, X. Liu, and L. Li, "A novel characteristic frequency bands extraction method for automatic bearing fault diagnosis based on Hilbert Huang transform," *Sensors*, vol. 15, no. 11, pp. 27869–27893, Nov. 2015.

[25] Y. Li, M. Xu, Y. Wei, and W. Huang, "An improvement EMD method based on the optimized rational Hermite interpolation approach and its application to gear fault diagnosis," *Measurement*, vol. 63, pp. 330–345, Mar. 2015.

[26] Y. Lei, J. Lin, Z. He, and M. J. Zuo, "A review on empirical mode decomposition in fault diagnosis of rotating machinery," *Mech. Syst. Signal Process.*, vol. 35, nos. 1–2, pp. 108–126, Feb. 2013.

[27] Y. Lei and M. J. Zuo, "Fault diagnosis of rotating machinery using an improved HHT based on EEMD and sensitive IMFs," *Meas. Sci. Technol.*, vol. 20, no. 12, Dec. 2009, Art. no. 125701.

[28] C. Yang and T. Wu, "Diagnostics of gear deterioration using EEMD approach and PCA process," *Measurement*, vol. 61, pp. 75–87, Feb. 2015.

[29] J. Cheng, K. Zhang, and Y. Yang, "An order tracking technique for the gear fault diagnosis using local mean decomposition method," *Mech. Mach. Theory*, vol. 55, pp. 67–76, Sep. 2012.

[30] J. Cheng, Y. Yang, and Y. Yang, "A rotating machinery fault diagnosis method based on local mean decomposition," *Digit. Signal Process.*, vol. 22, no. 2, pp. 356–366, Mar. 2012.

[31] X. Hu, S. Peng, and W.-L. Hwang, "EMD revisited: A new understanding of the envelope and resolving the mode-mixing problem in AM-FM signals," *IEEE Trans. Signal Process.*, vol. 60, no. 3, pp. 1075–1086, Mar. 2012.

[32] W.-C. Shen, Y.-H. Chen, and A.-Y. Wu, "Low-complexity sinusoidal-assisted EMD (SAEMD) algorithms for solving mode-mixing problems in HHT," *Digit. Signal Process.*, vol. 24, pp. 170–186, Jan. 2014.

[33] J. Zheng, J. Cheng, and Y. Yang, "Partly ensemble empirical mode decomposition: An improved noise-assisted method for eliminating mode mixing," *Signal Process.*, vol. 96, pp. 362–374, Mar. 2014.

[34] L. Zhang, Z. Wang, and L. Quan, "Research on weak fault extraction method for alleviating the mode mixing of LMD," *Entropy*, vol. 20, no. 5, p. 387, May 2018.

[35] K. Dragomiretskiy and D. Zosso, "Variational mode decomposition," *IEEE Trans. Signal Process.*, vol. 62, no. 3, pp. 531–544, Feb. 2014.

[36] F. Li, R. Li, L. Tian, L. Chen, and J. Liu, "Data-driven time-frequency analysis method based on variational mode decomposition and its application to gear fault diagnosis in variable working conditions," *Mech. Syst. Signal Process.*, vol. 116, pp. 462–479, Feb. 2019.

[37] S. Hu, H. Xiao, and C. Yi, "A novel detrended fluctuation analysis method for gear fault diagnosis based on variational mode decomposition," *Shock Vibrat.*, vol. 2018, pp. 1–11, Oct. 2018.

[38] K. Li, L. Su, J. Wu, H. Wang, and P. Chen, "A rolling bearing fault diagnosis method based on variational mode decomposition and an improved kernel extreme learning machine," *Appl. Sci.*, vol. 7, no. 10, p. 1004, Sep. 2017.

[39] J. Li, H. Wang, J. Zhang, X. Yao, and Y. Zhang, "Impact fault detection of gearbox based on variational mode decomposition and coupled underdamped stochastic resonance," *ISA Trans.*, vol. 95, pp. 320–329, Dec. 2019.

[40] X. Jiang, C. Shen, J. Shi, and Z. Zhu, "Initial center frequency-guided VMD for fault diagnosis of rotating machines," *J. Sound Vib.*, vol. 435, pp. 36–55, Nov. 2018.

[41] Z. Wang, J. Wang, and W. Du, "Research on fault diagnosis of gearbox with improved variational mode decomposition," *Sensors*, vol. 18, no. 10, p. 3510, Oct. 2018.

[42] Y. Miao, M. Zhao, Y. Yi, and J. Lin, "Application of sparsity-oriented VMD for gearbox fault diagnosis based on built-in encoder information," *ISA Trans.*, to be published.

[43] C. Wang, H. Li, G. Huang, and J. Ou, "Early fault diagnosis for planetary gearbox based on adaptive parameter optimized VMD and singular kurtosis difference spectrum," *IEEE Access*, vol. 7, pp. 31501–31516, 2019.

[44] X. Yan and M. Jia, "Application of CSA-VMD and optimal scale morphological slice bispectrum in enhancing outer race fault detection of rolling element bearings," *Mech. Syst. Signal Process.*, vol. 122, pp. 56–86, May 2019.

[45] X. Zhang, Q. Miao, H. Zhang, and L. Wang, "A parameter-adaptive VMD method based on grasshopper optimization algorithm to analyze vibration signals from rotating machinery," *Mech. Syst. Signal Process.*, vol. 108, pp. 58–72, Aug. 2018.

[46] C. Yi, Y. Lv, and Z. Dang, "A fault diagnosis scheme for rolling bearing based on particle swarm optimization in variational mode decomposition," *Shock Vib.*, vol. 2016, pp. 1–10, Jun. 2016.

[47] D. Han, N. Zhao, and P. Shi, "Gear fault feature extraction and diagnosis method under different load excitation based on EMD, PSO-SVM and fractal box dimension," *J. Mech. Sci. Technol.*, vol. 33, no. 2, pp. 487–494, Feb. 2019.

[48] S. Ma, B. Cheng, Z. Shang, and G. Liu, "Scattering transform and LSPTSVM based fault diagnosis of rotating machinery," *Mech. Syst. Signal Process.*, vol. 104, pp. 155–170, May 2018.

[49] M. Kuai, G. Cheng, Y. Pang, and Y. Li, "Research of planetary gear fault diagnosis based on permutation entropy of CEEMDAN and ANFIS," *Sensors*, vol. 18, no. 3, p. 782, Mar. 2018.

[50] Z.-X. Yang, X. Wang, and P. K. Wong, "Single and simultaneous fault diagnosis with application to a multistage gearbox: A versatile dual-ELM network approach," *IEEE Trans. Ind. Inf.*, vol. 14, no. 12, pp. 5245–5255, Dec. 2018.

[51] Y. Li, G. Cheng, C. Liu, and X. Chen, "Study on planetary gear fault diagnosis based on variational mode decomposition and deep neural networks," *Measurement*, vol. 130, pp. 94–104, Dec. 2018.

[52] P. Cao, S. Zhang, and J. Tang, "Preprocessing-free gear fault diagnosis using small datasets with deep convolutional neural network-based transfer learning," *IEEE Access*, vol. 6, pp. 26241–26253, 2018.

[53] R. Liu, B. Yang, E. Zio, and X. Chen, "Artificial intelligence for fault diagnosis of rotating machinery: A review," *Mech. Syst. Signal Process.*, vol. 108, pp. 33–47, Aug. 2018.

[54] D. F. Specht, "Probabilistic neural networks," *Neural Netw.*, vol. 3, no. 1, pp. 109–118, Jan. 1990.

[55] H. Liu, J. Jing, and J. Ma, "Fault diagnosis of electromechanical actuator based on VMD multifractal detrended fluctuation analysis and PNN," *Complexity*, vol. 2018, pp. 1–11, Aug. 2018.

[56] A. P. Marugán, F. P. G. Márquez, J. M. P. Perez, and D. Ruiz-Hernández, "A survey of artificial neural network in wind energy systems," *Appl. Energy*, vol. 228, pp. 1822–1836, Oct. 2018.

[57] R. Eberhart and J. Kennedy, "Particle swarm optimization," in *Proc. IEEE Int. Conf. Neural Netw.*, vol. 4, Nov. 1995, pp. 1942–1948.

[58] J. Sun, Q. Xiao, J. Wen, and F. Wang, "Natural gas pipeline small leakage feature extraction and recognition based on LMD envelope spectrum entropy and SVM," *Measurement*, vol. 55, pp. 434–443, Sep. 2014.

[59] J. S. Richman, D. E. Lake, and J. R. Moorman, "Sample entropy," *Methods Enzymol.*, vol. 384, pp. 172–184, Jan. 2004.

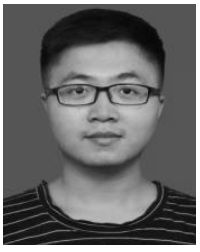

JIAKAI DING was born in Jiangxi, China, in 1996. He received the B.S. degree from the School of Mechanical and Electronic Engineering, East China University of Technology, Nanchang, China, in 2018. He is currently pursuing the M.S. degree with the School of Mechanical Engineering, Hunan University of Science and Technology. His current research interests include in-suit monitoring and fault diagnosis of equipment and additive manufacturing.

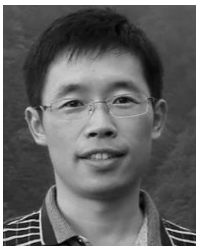

DONGMING XIAO was born in Hunan, China, in 1980. He received the B.S. and M.S. degrees in mechatronic engineering from the Hunan University of Science and Technology, in 2003 and 2008, respectively, and the Ph.D. degree in mechatronic engineering from the South China University of Technology, in 2013.

He was promoted to a Lecturer with the School of Mechatronic Engineering, Hunan University of Science and Technology, in 2009, then shifted to the Engineering Research Center of Advanced Mine Equipment, Ministry of Education, where he was an Associate Professor, in 2015. Since 2017, he has been an Academic Visitor with the University of Nottingham. He has been an Associate Professor with the School of Mechatronics Engineering, Foshan University, since 2019. He is the author of one book, more than 20 articles, and more than ten inventions. His research interests include in-suit monitoring and control of electromechanical equipment and additive manufacturing machine.

XUEJUN LI was born in Hunan, China, in 1969. He received the B.S. degree in mechanical engineering from the Hunan University of Science and Technology, in 1991, and the Ph.D. degree in mechanical engineering from Central South University, in 2003. He did his Postdoctoral research with Tsinghua University, China, from 2005 to 2009.

From 1997 to 2003, he shifted and promoted to a Lecturer and an Associate Professor with the School of Mechatronic Engineering, Hunan University of Science and Technology, where he was a Professor, in 2005. He has been a Professor with the School of Mechatronics Engineering, Foshan University, since 2019. He is the author of two books, and more than 100 articles 50 inventions. His research interests focus on health maintenance and fault diagnosis of equipment.